CRYPTOMARE, LAVA LAKES, AND PYROCLASTIC DEPOSITS IN THE GASSENDI REGION OF THE MOON: FINAL RESULTS. B.R. Hawke[1], T.A. Giguere[1,2], C.A. Peterson[1], S.J. Lawrence[3], J.D. Stopar[3], and L.R. Gaddis[4]. [1]Hawaii Institute of Geophysics and Planetology, University of Hawaii, Honolulu, HI 96822, [2]Intergraph Corporation, P.O. Box 75330, Kapolei, HI 96707, [3]School of Earth and Space Exploration, Arizona State University, Tempe, AZ 85281, [4]U.S. Geological Survey, Astrogeology Science Center, Flagstaff, AZ 86001.

Introduction: Gassendi is a floor-fractured impact crater (diameter = 110 km) located just north of Mare Humorum on the western nearside of the Moon. The Gassendi region contains a number of unusual features which have long provoked controversy. These include smooth plains and possible volcanic constructs on the floor of Gassendi [1,2], a large radar anomaly west of the crater [3], possible pyroclastic deposits in Mersenius crater, and a cryptomare deposit [3]. We have analyzed Lunar Reconnaissance Orbiter Camera (LROC) Wide Angle Camera (WAC) and Narrow Angle Camera (NAC) images, as well as a variety of other spacecraft data, to investigate the composition and origin of geologic units in the Gassendi region. The goals of this study include the following: 1) To determine the origin of possible volcanic features on the floor of Gassendi, 2) To search for cryptomare deposits and to investigate the processes responsible for their formation, 3) To determine the compositions and ages of any buried mare units, and 4) To investigate the distribution and compositions of pyroclastic deposits.

Methods: Both LROC WAC and NAC images were utilized in this investigation. The high resolution (0.5 m/pixel) provided by the NAC images was critical for the study of the smallest volcanic features. Topographic data were provided by the LROC GLD100 [7]. The U.S.G.S. Astrogeology Program has published on CD-ROM a Clementine five-color UV-VIS digital image model (DIM) for the Moon [e.g., 4]. Images from this DIM were used to produce an image cube centered on the Gassendi area. This calibrated image cube served as the basis for the production of a number of other data products, including optical maturity (OMAT) images and FeO and TiO_2 maps [5,6]. Five-point spectra were extracted from the calibrated and registered Clementine UV-VIS image cube.

Results and Discussion:

Pyroclastic Deposits. A previously unmapped dark mantle deposit of probable pyroclastic origin was identified in the highlands northeast of Gassendi. Dark material mantles and subdues underlying highland terrain. In places, it is draped over rugged mountain ridges. The deposit covers ~250 km^2 and is centered at 14.8°S, 37.7°W. A probable source vent has been identified using LROC images (Figure 1). This endogenic crater is associated with a linear rille and has an average diameter of 2.5 km and an average depth of 88 m. Two five-point spectra extracted for the dark material indicate that the deposit is dominated by mare basalt fragments and contains minor amounts of highland debris. In addition, the dark materials exhibit enhanced FeO and TiO_2 values.

Several localized pyroclastic deposits have been identified along fractures on the floor of Mersenius crater [3,13,14]. Five-point spectra collected for two pyroclastic deposits on the northwestern portion of the crater floor indicate a basaltic composition.

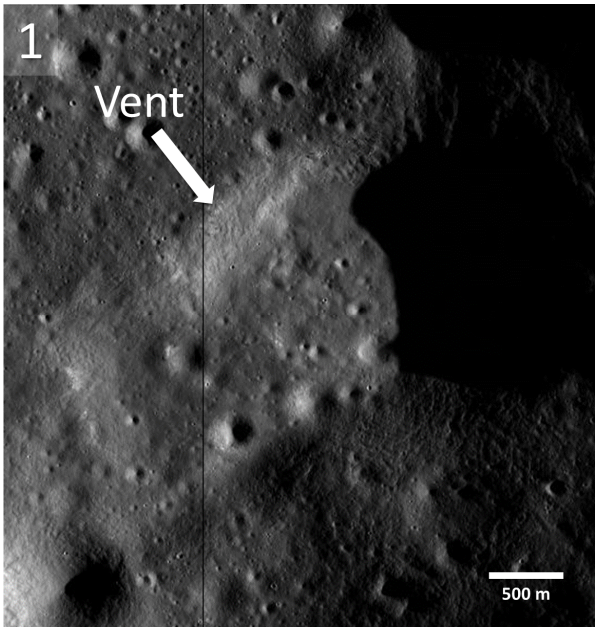

Figure 1. *Portion of a mosaic of NAC frames M193203275L&R. The pyroclastic vent is indicated by the white arrow. North is up.*

Gassendi Crater Interior. While mare basalt deposits have been identified in the southern, southeastern, and southwestern portions of the Gassendi interior [e.g., 1,2,8,9,10,11,12], no mare units have been mapped in the west central and northwestern portions of the crater floor. However, Schultz [1] described several features of possible endogenic origin in the NW portion of the floor. These included an irregular depression partly surrounded by a scarp which may be a lava terrace. Large parts of the west central and NW floor exhibit FeO values (12-14 wt.%) that are higher than those of the surrounding floor material (8-12 wt.%). A number of small impact craters excavated even more FeO-rich material. These craters range from 1 to 1.4 km in diameter, and LROC images show that

they have very faint dark haloes. The maximum FeO abundances measured for the dark haloes range from 14.4 to 14.8 wt.%. These values fall within the range of FeO abundances (14-18 wt.%) determined for the mapped mare units in the southern, SE, and SW portions of the crater floor. Five-point spectra were extracted from the Clementine UV-VIS image cube for two of the dark-haloed impact craters (DHCs). These spectra have moderately strong "1µm" bands centered near 0.95 µm. The materials for which these spectra were obtained have mafic assemblages dominated by high-Ca clinopyroxene. Both the chemical and spectral data indicate that mare basalts were exposed by DHCs on the western portions of the Gassendi crater floor. Mare basalt flows were emplaced in parts of the western floor and, later, were obscured by highlands-rich ejecta from Gassendi A and other craters, and a cryptomare deposit was formed.

Schultz [1,2] also described features of possible volcanic origin in the northeastern floor of Gassendi. These included high-level lava marks within fractures, and perched plains units. LROC NAC images show a terraced depression which may represent a drained lava lake (Figure 2). The region with these possible volcanic features exhibits enhanced FeO and TiO_2 values. The FeO abundances range from 12 to 16 wt.%. The highest FeO concentrations (14-16 wt.%) are associated with perched plains deposits NE and SW of Rima Gassendi II. These perched plains have a relatively low albedo and enhanced TiO_2 abundances (2-3 wt.%). This area corresponds to the ST spectral unit defined by Chevrel and Pinet [8,9] on the basis of Earth-based telescopic multispectral images. They determined that clinopyroxene was a major component in the ST material.

We collected five-point spectra from the Clementine image cube for four fresh surfaces associated with fracture walls and lava terrace scarps in the FeO-rich portion of the NE floor. These spectra exhibit strong "1µm" bands centered at or longward of 0.95µm. The lithologies for which these spectra were collected clearly contain large amounts of pyroxene and have mafic assemblages dominated by high-Ca clinopyroxene. These fracture walls and terrace scarps are dominated by mare basalt fragments. The results of previous studies [1,2,10,11] as well as the chemical and spectral data presented in this study indicate that mare volcanism occurred in the NE portion of the floor of Gassendi crater. These mare surfaces were contaminated and obscured by non-mare debris from Gassendi A and other craters in the surrounding highlands, and cryptomare deposits were formed.

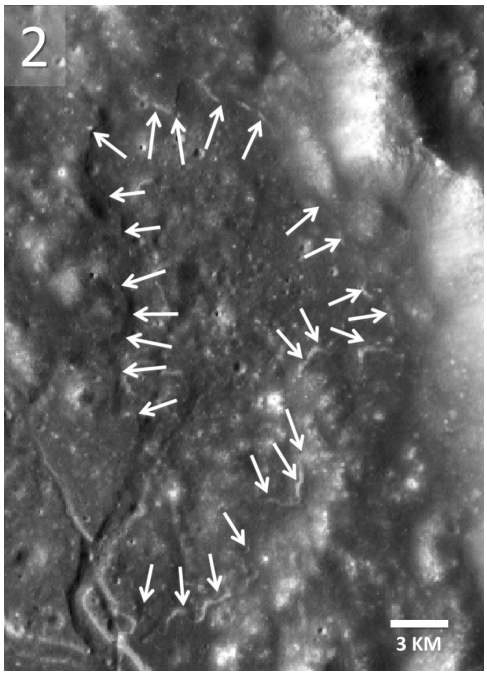

Figure 2*. Portion of a mosaic of NAC frames M193210370L&R. Arrows indicate a lava terrace. North is up.*

Lava Lakes in Gassendi. As discussed in the previous section, evidence exists for drained lava lakes on the floor of Gassendi. LROC images show that well-developed lava terraces occur on all sides of the northeastern drained lake (Figure 2). Topographic data show that the elevation of the terrace top changes as a function of position around the depression with elevations increasing to the south. Apparently, structural adjustments in the crater floor resulted in uplift of the southern portion of the drained lake. The maximum depth of the lava lake was at least 200 m. The NW drained lake exhibits a lava terrace along its southern edge. The elevation of the terrace top is constant along its exposed length. The maximum depth of this lake was ~90 m. A third lake existed on the SW portion of the crater floor. A lava terrace was identified at one location in this area.

References: [1] Schultz P. (1976) *Moon Morphology*, 626. [2] Schultz P. (1976) *Moon, 15*, 241. [3] Hawke B. *et al.* (1993) *GRL, 20*, 419. [4] Eliason E. *et al.* (1999) *LPS XXX*, #1933. [5] Lucey P. *et al.* (2000) *JGR, 105* (E8), 20,297. [6] Lucey P. *et al.* (2000) *JGR, 105* (E8), 20,377. [7] Scholten F. *et al.* (2012) *JGR, 117*, 12 pp. [8] Chevrel S. and Pinet P. (1990) *PLPSC 20*, 187. [9] Chevrel S. and Pinet P. (1992) *PLPSC 22*, 249. [10] Hiesinger H. *et al.* (2000) *JGR, 105* (E12), 29,239. [11] Hackwill T. *et al.* (2006) *MAPS, 41*, 479. [12] Titley S. (1967) U.S.G.S. Map I-495. [13] Gaddis L. *et al.* (2003) *Icarus, 161*, 262. [14] Gustafson O. *et al*. (2014*) LPSC XLV*, #2044.